

FLUID MECHANICS OF CO-CURRENT TWO-PHASE FLOW IN PACKED BEDS: PRESSURE DROP AND LIQUID HOLDUP STUDIES*

By

Mahmoud Y. SAADA

Pilot Plant Laboratories, National Research Centre Dokki, Cairo, U.A.R.

(Received February 17, 1974)

Introduction

A main factor required for the design of packed columns is the knowledge of the mechanism of flow inside the pores which is basic to an interpretation of the interfacial areas available for mass transfer.

FORD [1, 2] reported the existence of two regimes of flow inside the pores, namely, the single-phase pore-flow and the two-phase pore-flow. It was found necessary to carry out experiments to confirm, over a wider experimental field, the existence of these two regimes of pore-flow before attempting any mass transfer studies [3].

This paper is a study of the fluid mechanics, pressure drop and liquid holdup, of co-current two-phase flow through a column packed with 0.514, 0.974 and 2.064 mm nominal diameter glass ballotini spheres when gas and liquid flow upwards in the turbulent regime.

No satisfactory theoretical method of analysis could be devised because the description of flow through the pores and also the micro parameters have not been fully theoretically evaluated. The porous mass consists of a network of interconnecting channels whose diameter and length vary to a great extent and it is, thus, difficult to define precisely the actual fluid path length and the spatial distribution of fluids over the cross section of the mass. To avoid the need to consider these parameters, the results were analysed empirically by dimensional analysis.

The glass ballotini spheres were packed in a 4.5 cm I.D. by 40 cm long vertical column to a porosity of 34.6%. The column was designed to operate at 200 p.s.i. and the two fluids were introduced at the bottom through a special gas-liquid distributor. The ranges of Reynolds numbers for liquid and gas, based on the superficial velocity of the fluid and the particle diameter, were 2 to 200, and 8 to 900, respectively.

* LECTURED BEFORE THE DEPARTMENT OF AGRICULTURAL CHEMICAL TECHNOLOGY, TECHNICAL UNIVERSITY BUDAPEST.

Previous work

Various attempts have been made to investigate two-phase flow in tubes in all possible flow configurations. Less has been done in the laminar regime of flow through porous masses, while only few attempts were made to correlate two-phase systems in packed beds where the two phases are flowing co-currently in the turbulent regime of flow.

Studies have mainly been concentrated on the correlation of pressure drop with other properties of the system, and to some extent on the determination of cross sectional holdup of the phases and the related differences in velocity.

The investigation of two-phase flow has been approached from two different viewpoints. The majority of investigators have set out the equations of motion and energy for single-phase flow and then attempted to modify particular variables in these equations to suit the simultaneous flow of two phases. The BROWNELL and KATZ friction chart analogy [4, 5, 6] comes within this classification. The second approach was to present a dimensionless correlation between all possible variables affecting the driving force inside the packed column. The work of SCHWARTZ [7] and FORD [1] comes within this classification. (The present work will indicate the feasibility of this approach.)

The recent work of FORD [1] was to use dimensional analysis in order to correlate the results obtained from a study of the co-current two-phase flow in beds packed with approximately 1 mm particle diameter. Most of his results were reanalysed statistically and by replotting, unsatisfactory correlations were obtained, particularly for the holdup lines. The value of his work is to identify two regimes of flow that take place inside the pores, namely, "single-phase pore-flow" and "two-phase pore-flow", and for each regime he introduced a dimensionless correlation. The two correlations are:

$$\frac{\Delta p}{\rho_L \Delta s} = 0.0407 (Re_L)^{0.29} (Re_G)^{0.57} (\eta_L/\eta_G)^{0.28} \quad (1)$$

for two-phase pore-flow, and

$$\frac{\Delta p}{\rho_L \Delta s} = 0.0485 (Re_L)^{0.67} (Re_G)^{0.3} (\rho_L/\eta_G)^{0.8} \quad (2)$$

for single-phase pore-flow. (Definitions see in NOTATIONS.)

The selection of the correct driving force equation was made by using Eq. (3) to predict the liquid holdup, ϑ ,

$$\vartheta = 21.2 (Re_L/Re_G)^{0.2} (\eta_L/\eta_G)^{0.24} \quad (3)$$

FORD reported that the value of liquid holdup at the transition point between one mode of flow and the other, θ_T , has a constant value of $43\% \pm 3\%$ for all gas and liquid Reynolds numbers. Hence, if values of θ , calculated from Eq. (3), are less than θ_T , Eq. (1) is to be used in order to calculate the pressure drop along the mass, while if $\theta > \theta_T$, Eq. (2) is to be used.

In the present work the value of θ_T was found experimentally to be a *variable*. This was checked analytically as follows: assuming that the three equations of FORD, (1), (2) and (3) are consistent, therefore at the transition point, the driving force will be the same in both regimes of pore flow. By equating Eqs (1) and (2), one gets:

$$(\eta_L/\eta_G)^{0.52} = 0.839 (Re_L)^{-0.38} (Re_G)^{0.27}$$

and by substituting in Eq. (3) for (η_L/η_G) ,

$$\theta_T = 17.8 (Re_L)^{0.02} (Re_G)^{0.08} \quad (4)$$

Now, substituting the maximum values of Re_L and Re_G that FORD has used, (150 and 1000, respectively), in Eq. (4):

$$\theta_T = 11.3\% \neq 43\%.$$

It was, thus, found necessary, to repeat part of FORD's work.

Experimental

General arrangements

Fig. 1 illustrates a schematic flow diagram of the system.

The high-pressure air supply to the packed column was obtained from a three-phase electric compressor discharging into a gas reservoir I, which helped to provide a continuous air flow and to maintain it, when required, at a maximum flow rate of 3 lbs/min, and a maximum pressure of 400 p.s.i.g. To avoid excessive pressure the reservoir was fitted with a bleed valve and a silencer k, which eliminates excessive noise produced by the escape of the excessive pressurized air. The air, then, passed through an impact separator j, packed with charcoal to free it from any entrained moisture and oil from the compressor. The air pressure, was, then, reduced to the maximum working pressure of the column, viz., 200 p.s.i.g., then part of it was metered by two rotameters R, connected in parallel to cover the required range of gas flow rates. This part was then passed to the distributor at the bottom of the column

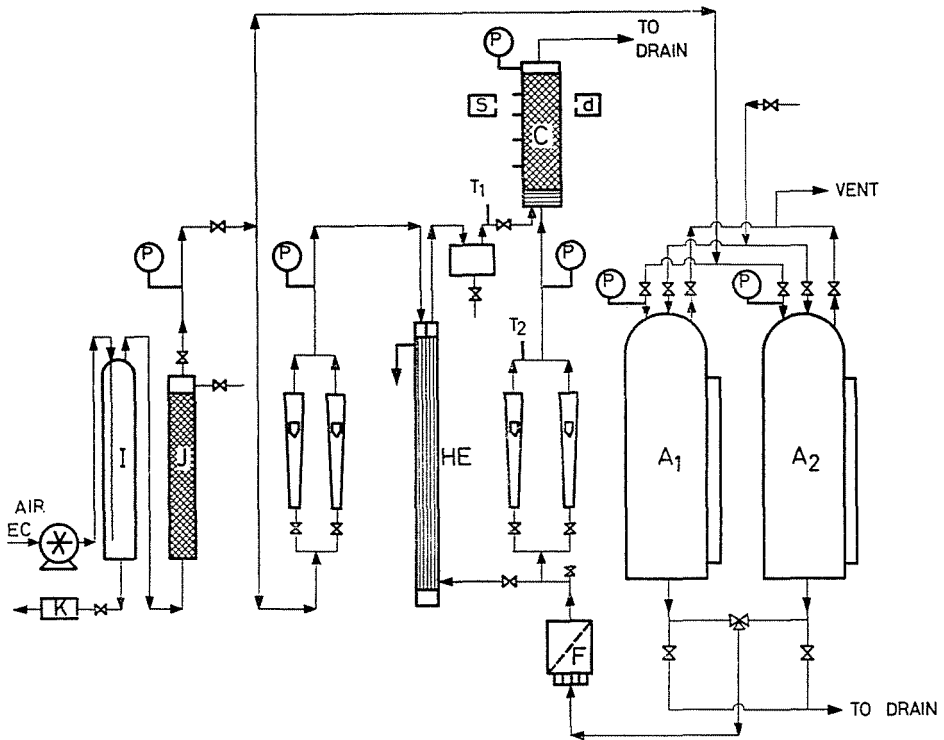


Fig. 1. Flow diagram of the two-phase system

via a heat exchanger HE, a catch pot and a non-return valve. The other part of air was utilized to pump water into the system, thus, providing a continuous supply of water from either of the two tanks A_1 or A_2 , while the other was being filled from the mains. The water, then, flows to the distributor of the column through a filter F, after being metered by a similar bank of two rotameters R, connected also in parallel. To confirm that, the two phases were flowing at the same temperature, part of the water, before metering, was passed counter-currently to the air stream into the heat exchanger HE. The temperature of either phase was measured by two thermometers T_1 and T_2 , while their flow rates were controlled by a series of valves. Pressure gauges P, were used to measure the pressure of each stream and also the change in pressure along the column.

The column

The column used was similar to that used by FORD [1]. It was approximately 40 cm long, 4.52 cm I.D., and consisted essentially of five brass and five perspex sections screwed together alternately. The porous mass height

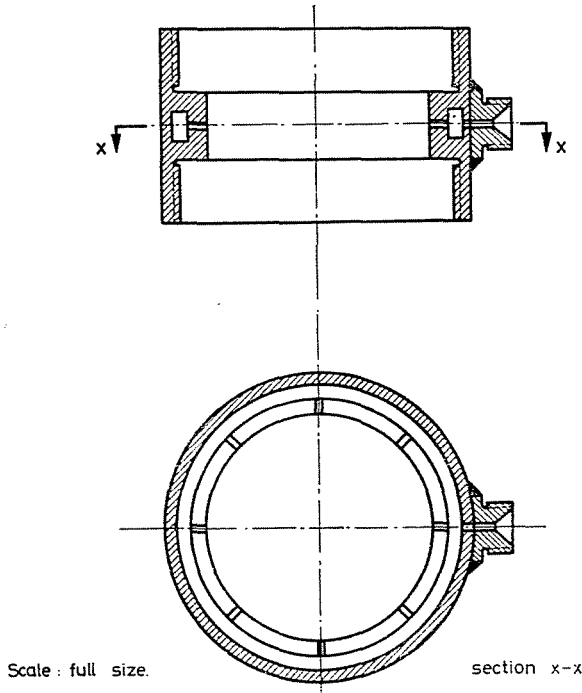


Fig. 2. The piezometer ring

of 37.3 cm was selected to investigate any variation of pressure drop and liquid holdups with length, while the choice of the column diameter, 4.52 cm, was governed by the criterion that the wall effect is negligible when the ratio of the tower diameter to the largest particle diameter used is greater than 40 to 50. The brass sections of the column consisted of piezometer rings, Fig. 2, which contained a central circumferential channel connected to the interior surface of the rings by eight $0.03'' \times 0.1''$ equally-spaced slots. These piezometer rings were designed to facilitate pressure measurements by giving an average circumferential pressure at the eight equally-spaced points. The perspex sections screwed into the piezometer rings giving a perfectly smooth inside surface to the column. Their function was to provide a medium through which the γ -rays could pass and be accounted for to assess the liquid holdup along the packed bed.

The packed material was held in position inside the column by two stainless steel wire gauzes at the extreme ends of the column with mesh smaller than the smallest particle diameter used.

The gas and liquid entered the bottom of the column through a specially designed distributor, recommended by HELSBY [8], and shown in Fig. 3.

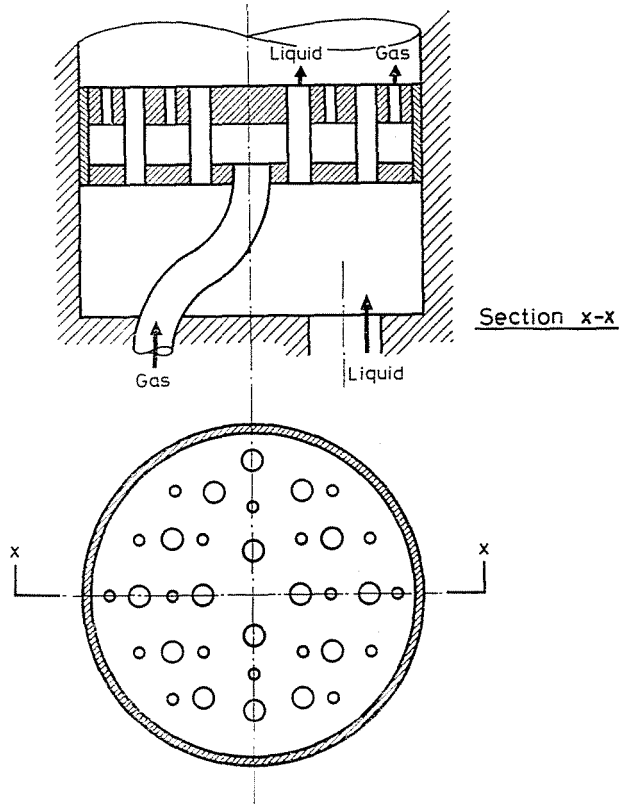


Fig. 3. Liquid and gas distributor

Analysis of results

The difficulty to establish a comprehensive theory to illustrate the mechanism of co-current two-phase flow in packed beds is partly due to the complexity of the structure of the porous mass. The porous mass is considered to consist of a network of interconnecting channels whose length and cross-sectional area vary between maximum and minimum values depending on the shape of the particles making up the mass. It is, thus, difficult to define precisely pore diameter, actual fluid path length, fluid velocity inside the pores and the distribution of the two phases over the cross section of the mass.

The proposed method of analysis has avoided the need to consider the above parameters by dimensional analysis. The driving force, expressed by the pressure gradient along the porous mass, and the liquid holdup, defined as the fraction of the porous mass occupied by the liquid phase, are correlated with parameters based on the macro dimensions of the mass, namely, the gas

and liquid Reynolds numbers, based on the superficial velocity of either phase and the ratio of the particle diameter to the container diameter.

The main objection to the application of dimensional analysis is that it does not lead to a complete understanding of the fundamental mechanisms of the process, but it is useful in the formulation of correlations for complicated processes which are difficult to treat theoretically.

Dimensional analysis is based on the assumption that the ratio of two similar quantities is independent of the units used. From this it follows that every derived quantity can be expressed as a constant multiplied by powers of the primary quantities.

A) Analysis of the driving force

For an upward co-current two-phase flow, the pressure drop representing the driving force, $\frac{\Delta p}{\rho_L g}$, was assumed to be affected by the following ten independent variables: G , L , d_p , d_t , Δs , ρ_L , η_L , η_G , γ and f . Equating the independent variables to the driving force and applying the Π -theorem, seven dimensionless groups are thus given, viz.,

$$\frac{\Delta p}{\rho_L g} k d_p Re_G^a Re_L^b We^c (d_p/d_t)^e (\Delta s/d_p)^h (\eta_L/\eta_G)^m (f)^q \quad (5)$$

where

$$Re_G = (G d_p/\eta_G), \quad Re_L = (L d_p/\eta_L) \quad \text{and} \quad We = (L^2 d_p/\rho_L \gamma)$$

Considering Eq. (5), the exponent h is unity since the pressure drop is directly proportional to the effective length of the mass Δs , see Appendix.

Since the viscosities of the gas and liquid as well as the bed porosity were kept constant throughout the present work, therefore the values of the two groups $(\eta_L/\eta_G)^m$ and $(f)^0$ will be accounted for by the equation constant. FORD [1] proved that for a case similar to the present one, the effect of Weber number was insignificant in studying the effect of liquid surface tension. Eq. (5), therefore, reduces to

$$\frac{\Delta p}{\rho_L g \Delta s} = K Re_G^a Re_L^b (d_p/d_t)^e \quad (6)$$

The values of the exponents: a , b , and e for each of the present two regimes of pore-flow are determined from the slope of the lines plotted from a least square regression and representing the variation of the driving force

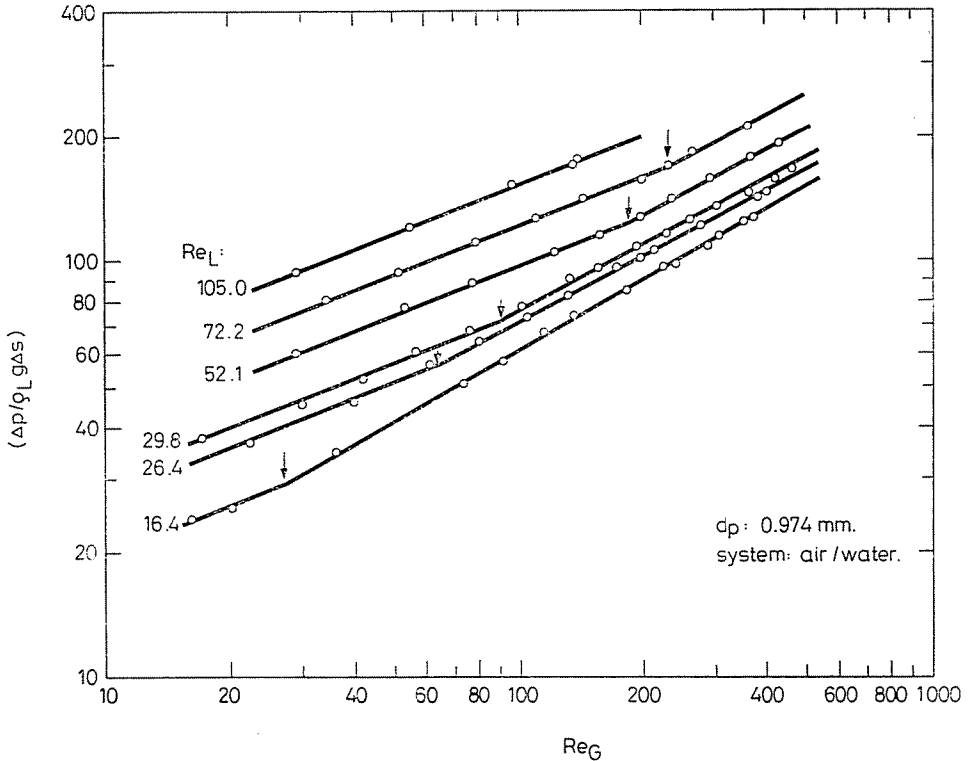


Fig. 4. Driving force vs. Re_G for different values of Re_L ($d_p = 0.974$ mm)

with either of the three dimensionless groups keeping the other two constant, Figs 4, 7 and 8, while the values of the constant K , in the correlation are calculated from Figs 9 and 10. The results are given in Table I:

Table I
Exponents in Eq. (6)

	Above transition			Below transition		
	a	b	c	a	b	e
Exponent	0.51	0.35	-1.15	0.39	0.60	-1.1
Variance of error of individual results	0.00002	0.0002	0.001	0.00004	0.0002	0.003
Variance of exponent	0.00007	0.001	0.0009	0.00005	0.001	0.0008
Correlation factor	0.998	0.989	-1.000	0.999	0.998	-0.995
Degrees of freedom	18	3	1	15	4	1

Eq. (6) can, thus, be written in the form:
for the regime below transition,

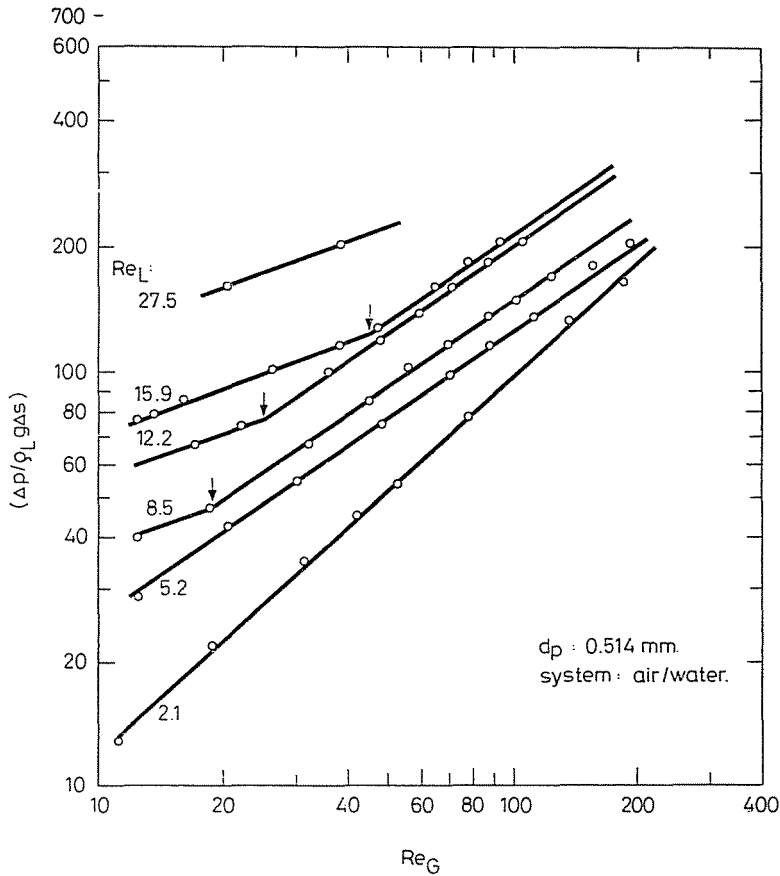


Fig. 5. Driving force vs. Re_G for different values of Re_L ($d_p = 0.514$ mm)

$$\frac{\Delta p}{\rho_L g \Delta s} = 0.024 Re_G^{0.39} Re_L^{0.60} (d_p/d_t)^{-1.1} \tag{7}$$

for the regime above transition,

$$\frac{\Delta p}{\rho_L g \Delta s} = 0.027 Re_G^{0.51} Re_L^{0.35} (d_p/d_t)^{-1.15} \tag{8}$$

B) Analysis of the liquid holdup

The correlation of the liquid holdup θ , in a packed column was tested in a way similar to that used for the driving force correlation, i.e., by using the method of dimensional analysis.

The liquid holdup θ , was assumed to be dependent on the independent variables G , L , η_G , η_L and f .

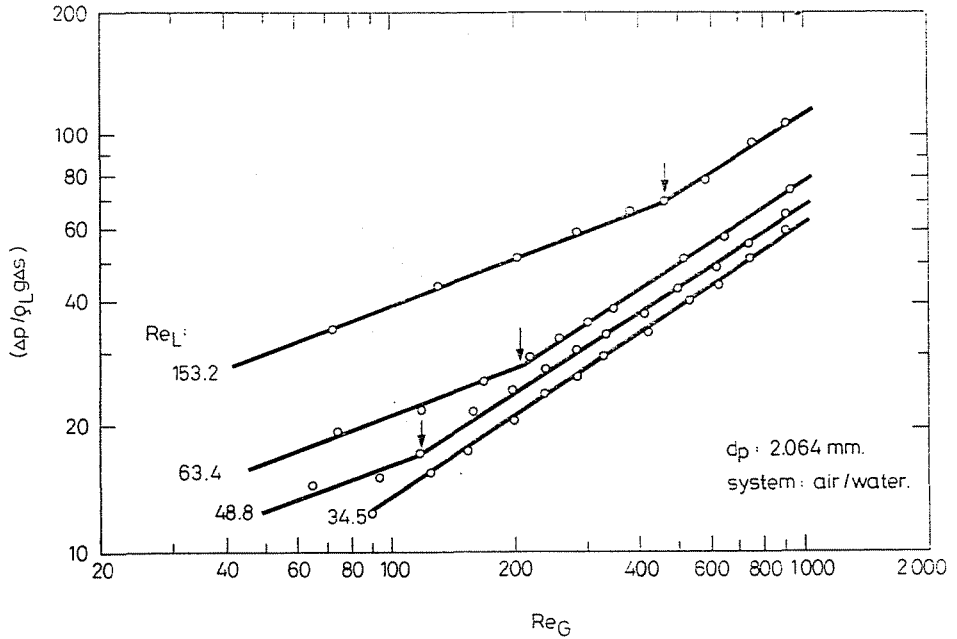


Fig. 6. Driving force vs. Re_G for different values of Re_L ($d_p = 2.064$ mm)

From dimensional analysis, and assuming that η_L , η_G and f are constant, one obtains:

$$\vartheta = K(Re_L/Re_G)^a. \quad (9)$$

The values of a and K for both regimes of pore-flow were obtained in a way similar to that used in the correlation of pressure drop; the results are compiled in Table II:

Table II
Exponents and constants in Eq. (9)

	Above transition		Below transition	
	a	K	a	K
Exponent or constant	0.07	0.32	0.25	0.48
Variance of error of individ. result	0.00002	0.0003	0.00002	0.0003
Correlation factor	0.979	0.894	0.995	0.916
Number of degrees of freedom	26	10	9	9

Eq. (9) can, thus, be written in the form:
for the regime below transition:

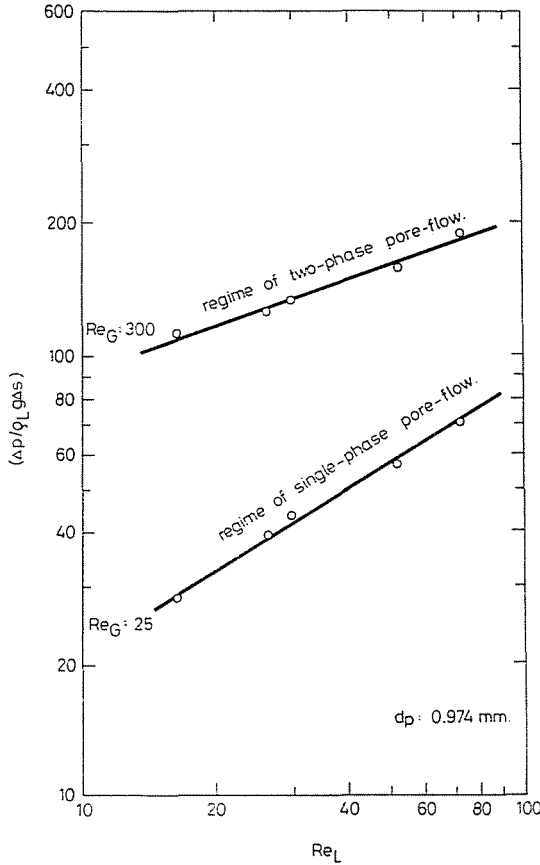


Fig. 7. Driving force vs. Re_L for different values of Re_G

$$\vartheta = 0.48 (Re_L/Re_G)^{0.25} \tag{10}$$

for the regime above transition:

$$\vartheta = 0.32 (Re_L/Re_G)^{0.07} \tag{11}$$

C) *Analysis of the transition point*

An equation representing the transition points from one regime of pore-flow to the other, can be postulated from the assumption that at the transition point, the driving force is the same in both regimes of flow. Thus, by equating Eqs (7) and (8):

$$Re_G^* = 0.44 Re_L^2 (d_p/d_i)^{0.38} \tag{12}$$

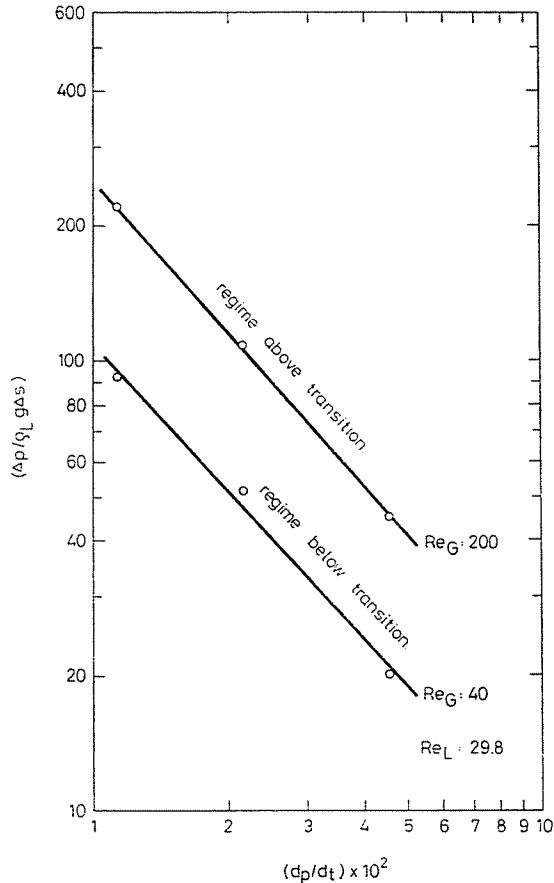


Fig. 8. Driving force vs. (d_p/d_t) for different values of Re_G

where Re_G^* is the gas Reynolds number at which transition occurs.

Eq. (12) can be used to predict which of the two regimes of flow is prevailing and, thus, the choice of the applicable driving force or liquid holdup equation is made.

Discussion of results

The effect of different experimental variables on the driving force, necessary to maintain the flow through the bed, has been studied. Fig. 4 shows the variation of the driving force $(\Delta p/\rho_L g \Delta s)$, with Re_G for different values of Re_L when the bed was packed with glass ballotini spheres of 0.974 mm nominal diameter. Figs 5 and 6 are similar to Fig. 4 except for the packing

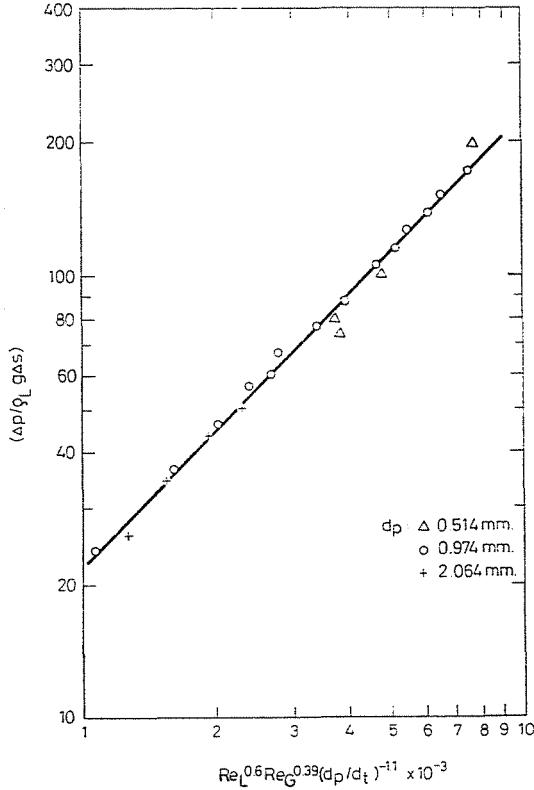


Fig. 9. Pressure drop correlation for the regime below transition

diameter, namely, 0.514 mm and 2.064 mm, respectively. From these three figures it is clear that the driving force increases linearly, on a log-log plot, with increase in the gas flow rate, until a point is reached where the slope of the lines of different values of Re_L shows an abrupt change. This point has been termed “The Transition Point” and the value of gas Reynolds number at which transition takes place has been termed “The Transition Gas Reynolds Number”, Re_G^* .

FORD [1] succeeded in predicting the existence of two regimes of pore-flow, namely, the regime of “Single-Phase Pore-Flow” below the transition point and the “Two-Phase Pore-Flow” above the transition point. The transition points in the present investigations differ considerably from those reported by FORD, while the slope of the lines giving the exponents of the pressure drop correlations differs to a lesser extent.

Fig. 7 shows the variation of the driving force with Re_L for two values of Re_G selected to represent each of the two regimes of pore-flow, while in Fig. 8 the variation of the driving force with (d_p/d_t) is shown for each regime. The exponent of the dimensionless group (d_p/d_t) in both regimes is approxi-

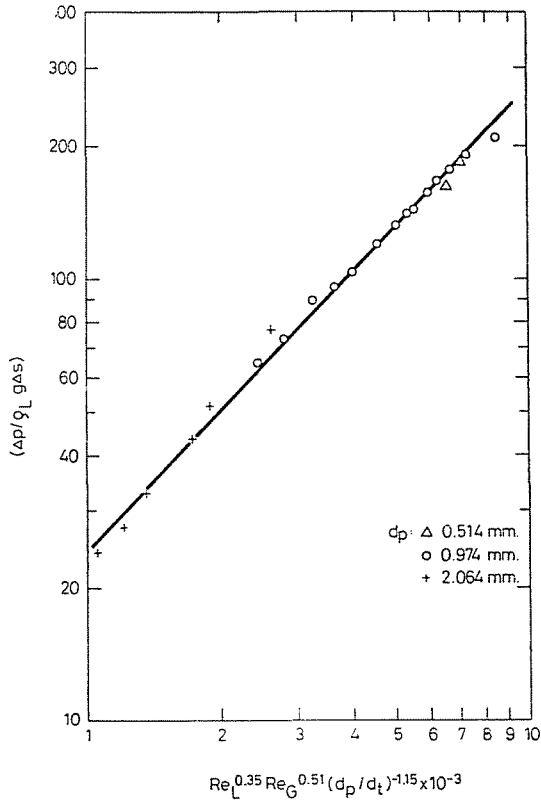


Fig. 10. Pressure drop correlation for the regime above transition

mately the same, indicating that the effect of the particle diameter is the same, regardless which of the two regimes prevails.

The final correlations of pressure drop, Eqs (7) and (8), are plotted in Figs 10 and 11, respectively. From these two plots the values of the constant K in the two correlations could also be estimated.

It is worth noting that both Eqs (7) and (8) are valid only when the two phases are flowing simultaneously through the bed since they suffer from the fact that when either of the two fluids ceases to flow the pressure drop becomes zero, which is not normally the case.

The liquid holdup studies on the bed, packed with 0.974 mm spheres, confirm the presence of the transition point and the values of Re_G^* in both Figs 4 and 11, for the same Re_L , are almost identical. Fig. 10 is a plot showing the variation of θ with Re_G for different values of Re_L .

In a way similar to that used to correlate the pressure drop results, two dimensionless correlations for liquid holdup are postulated, the exponent and

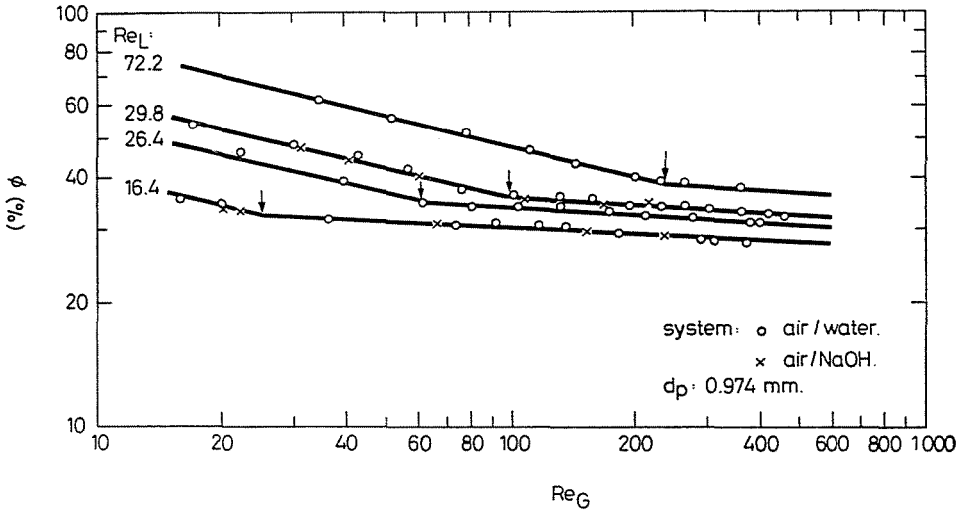


Fig. 11. Liquid holdup, ϕ , vs. Re_G for different values of Re_L

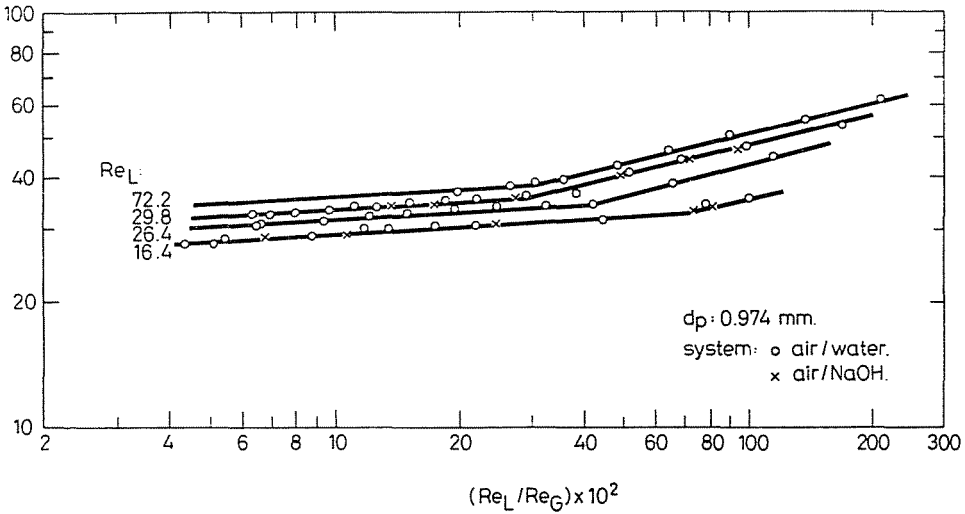


Fig. 12. Liquid holdup, ϕ , vs. (Re_L/Re_G) for different values of Re_L

constant of each are calculated from Fig. 12 which shows the change in ϕ with various values of (Re_L/Re_G) for different values of Re_L .

The selection of the correct driving force or liquid holdup equation corresponding to the prevailing regime of pore-flow can either be made by using Eq. (12) to calculate Re_G^* or from a plot, Fig. 13, similar to that used by LOBO et al. [9] to predict the onset of flooding in a packed tower. They

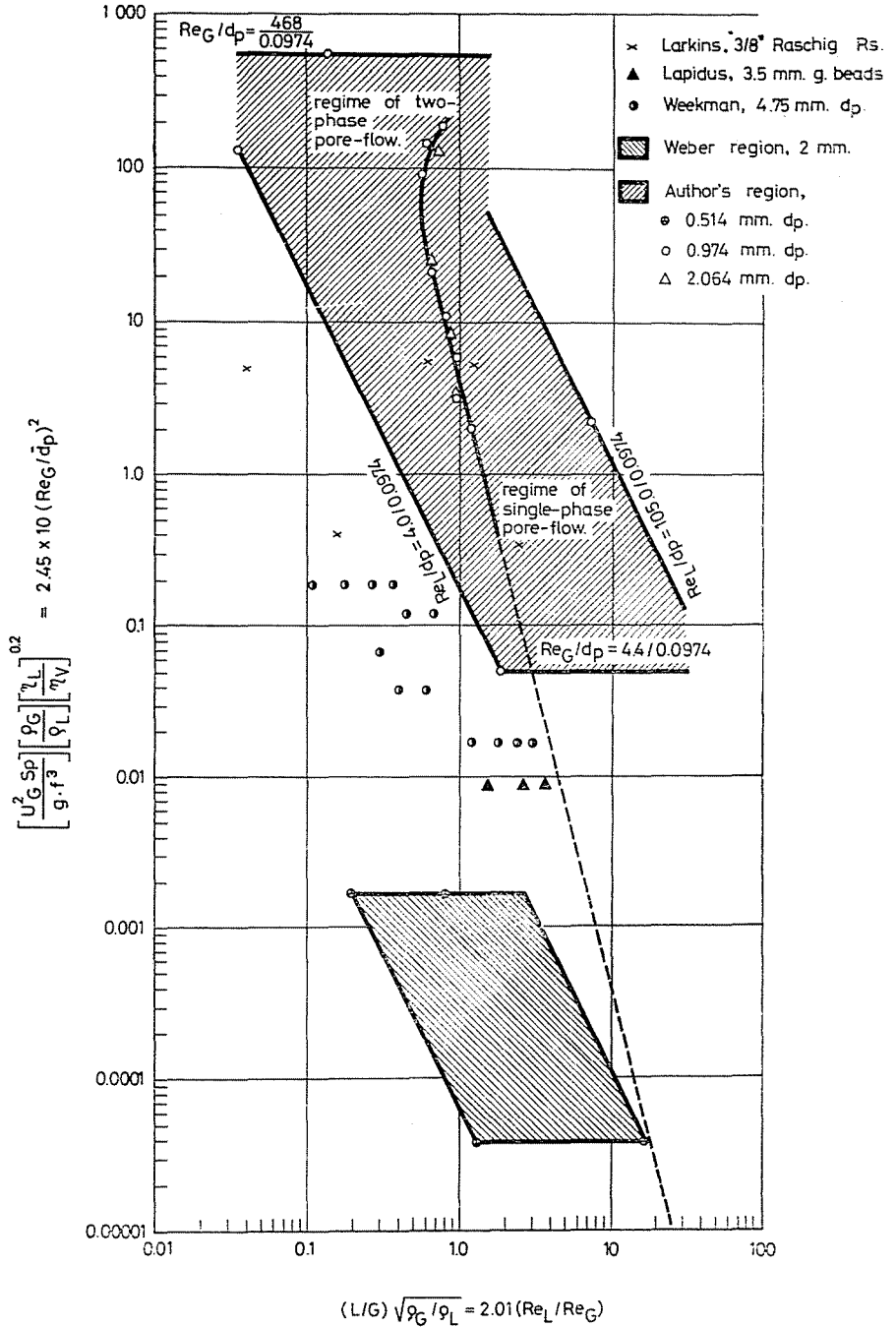


Fig. 13. A correlation for transition

obtained the operating boundary by correlating the two dimensionless expressions: (definitions see in NOTATIONS)

$$\frac{u_G^2 S_p}{gf^3} (\rho_G/\rho_L) (\eta_L/\eta_G)^{0.2} \quad \text{and} \quad (L/G) \sqrt{\rho_G/\rho_L}$$

It is suggested that the same dimensionless expressions can be used to obtain the transition boundary between the two regimes of pore-flow. For the system studied, the above expressions reduce to the following: $2.45 \times 10^{-5} (Re_G/d_p)^2$ and $2.01 (Re_L/Re_G)$.

In Fig. 13, the boundary curve is produced by plotting the values of the transition points for different particle diameters, shown in Figs 4, 5, 6 and 11, while the experimental universe is indicated by lines of maximum and minimum Reynolds numbers for water and air. The experimental points of the regime of single-phase pore-flow lie in the area below the transition curve while those of the regime of two-phase pore-flow lie in the area above the transition curve and within the experimental universe. Thus, knowing the values of Re_G , Re_L and d_p , a point can be located in either of the two defined areas in Fig. 13, indicating which regime is prevailing and consequently which equation to be used in order to calculate the pressure drop and the liquid holdup. Results of other investigators [10, 11, 12, 13] are also shown in Fig. 13 for different sizes and shapes of packings. Most of these results lie in the region where two-phase pore-flow occurs and this explains the reason why no kink points have been accounted for in their observations.

It is also noted from Fig. 13 that at a constant gas flow rate, an increase in the liquid flow rate will bring about transition to single-phase pore-flow but there appears to be an upper limit to the gas rate beyond which only two-phase pore-flow is possible. Conversely, at a constant liquid rate a decrease in the gas flow rate will bring about single-phase pore-flow.

The mechanism of flow inside the pores has been studied by EISENKLAM and FORD [2] who concluded that in the regime below transition, the two phases flowed through different pores; single-phase pore-flow, while in the regime above transition, the two phases flowed through the same pores; two-phase pore-flow.

APPENDIX

Preliminary studies

It was found necessary to carry out preliminary experiments to establish the uniformity of packing and the variation of pressure and liquid holdup along the porous mass.

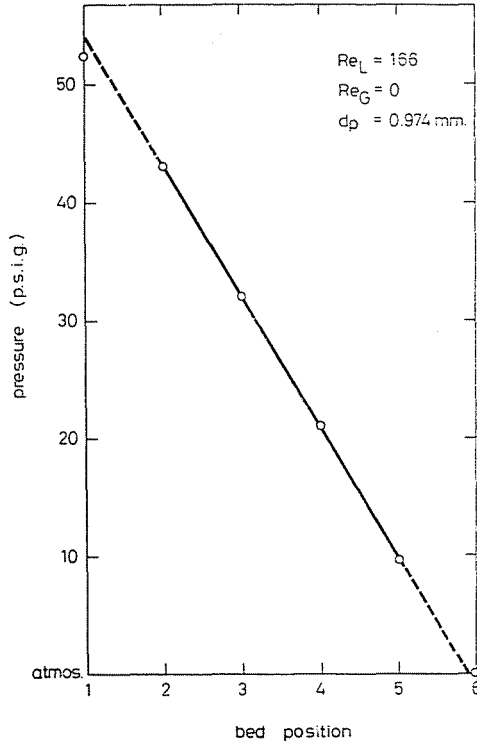


Fig. 14. Pressure distribution along the fully saturated mass

Uniformity of packing. This was tested by saturating the mass completely with water at a constant liquid flow rate and pressure readings were taken at each of the five piezometer rings of the column. The results shown in Fig. 14 indicate that the porosity of the mass was slightly different at both the upstream and the downstream ends than at the intermediate part of the bed between pressure tappings 2 and 5. Since the driving force to maintain a given flow rate through the bed is very sensitive to changes in porosity, only the length of the mass between pressure tappings 2 and 5 was considered.

A radiological technique was used to check the above results, and also to check the uniformity of packing across the cross sectional area of the mass by measuring the amount of radiation absorbed along different diameters of the mass. This was achieved by rotating both the source and counter around the axis of the column at different levels along the mass using the positioning and traversing devices [14]. This was found to be constant, as shown in Fig. 15.

Variation of pressure and holdup along the mass. Fig. 16 shows the variation of the pressure and liquid holdup measured at equidistant positions along the length of the porous mass for two combinations of Re_L and Re_G .

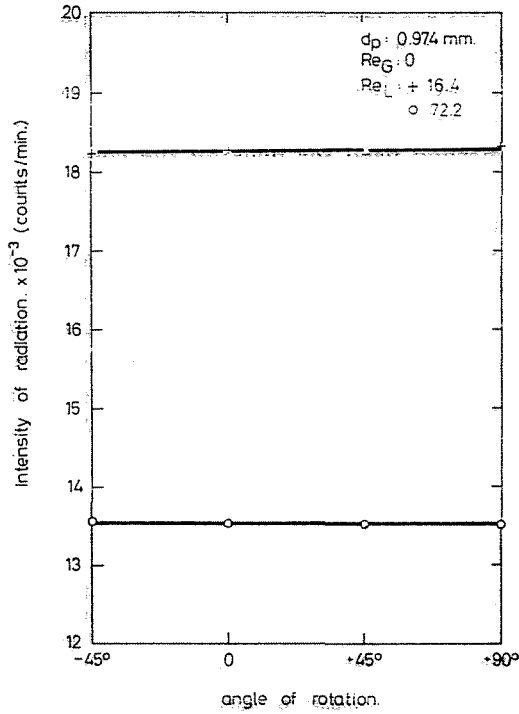


Fig. 15. Uniformity of packing across the bed

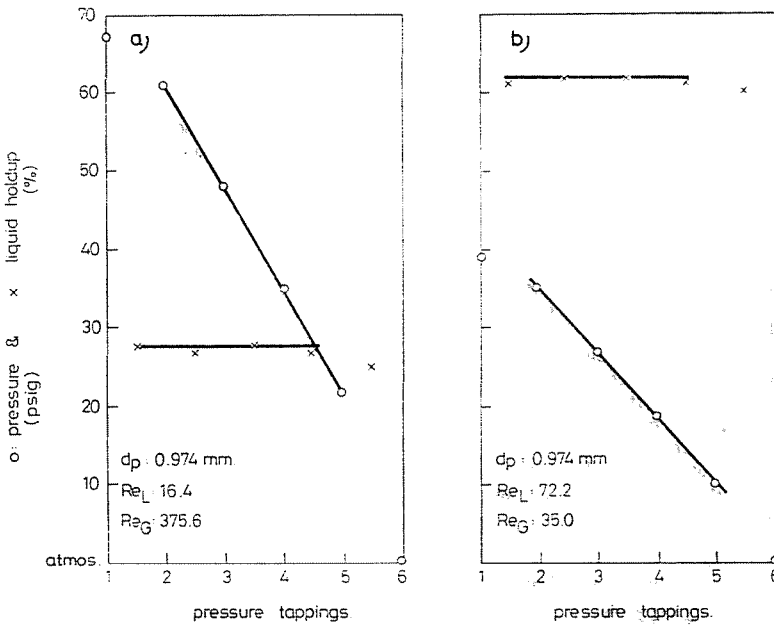


Fig. 16. Pressure and liquid holdup distribution along the bed

Except for the pressure readings from the two tappings 1 and 6, the pressure gradient remained essentially constant along the effective length of the mass, between tappings 2 and 5, hence compressibility effects could be neglected. The deviation of the results from the two end tappings is attributed to the end effects due to the method used for packing the column.

The results of the liquid holdup indicate that for constant gas and liquid flow rates the amount of liquid inside the pores remains constant along the porous mass. A further evidence of the end effect is given by the decline in holdup in the end portion of the bed (between tappings 5 and 6). Such decline is attributed to an increase in porosity at the end part of the bed.

The variation of the liquid holdup across the porous mass has been studied by rotating the γ -radiation source and detector around the axis of the column. The results prove that the liquid holdup is always constant across the bed.

Summary

A study of the fluid mechanics of the co-current flow of gas and liquid mixtures through beds of 1 mm spheres had revealed two regimes of flow inside the pores which were interpreted on the basis of two flow configurations, one where the pores were predominantly in single-phase flow and the other where they were predominantly in two-phase flow.

These regimes have been identified on beds with other packings and the interpretation checked by means of liquid holdup measurements using a γ -radiation absorption technique.

Correlations based on dimensional analysis for pressure drop and liquid holdup for each of the two regimes are given. An equation, to select the correct correlation for the existing regime has also been reported.

NOTATIONS

- Δp : Pressure differential along the porous mass, (gm/cm.sec²)
 Δs : Distance of the mass across which pressure was measured, (cm)
 Re : Reynolds number, (—)
 We : Weber number, (—)
 d : Diameter, (mm)
 f : Porosity, (—)
 g : Gravity acceleration, (cm/sec²)
 G : Specific gas flow rate, (gm/cm² sec)
 L : Specific liquid flow rate, (gm/cm² sec)
 K : Constant
 u : Superficial velocity, (cm/sec)
 S_p : Specific surface, (cm⁻¹)
 a, b, e : Exponents in Eq. (6)
 θ : Liquid holdup, (—)
 ρ : Density, (gm/cm³)
 η : Viscosity, (gm/cm. sec)
 γ : Interfacial tension, (gm/sec²)
Superscript: *: Value at transition
Subscripts: L: Liquid
 G: Gas
 T: Transition value
 t: Container
 p: Packing
 w: Water

References

1. FORD, L. H.: Multiphase Flow through Porous Media, with Special Reference to the Turbulent Regime. Ph. D. Thesis. Univ. of London (1960)
2. EISENKLAM, P.—FORD, L. H.: Proc. of the Symp. on the Interaction between Fluids and Particles. Inst. Chem. Engrs., June (1962), 333
3. SAADA, M. S. Y.: Co-Current Two-Phase Flow in Packed Beds, with Special Reference to Gas Absorption. Ph. D. Thesis. Univ. of London (1965)
4. BROWNELL, L. E.—KATZ, D. L.: Chem. Eng. Progr. **43**, 537 (1947)
5. BROWNELL, L. E.—KATZ, D. L.: Chem. Eng. Progr. **43**, 601 (1947)
6. BROWNELL, L. E.—DOMBROWSKI, H. S.—DICKEY, C. A.: Chem. Eng. Progr. **46**, 415 (1950)
7. SCHWARTZ, N.: De Ingenieur **68 MA** (1956)
8. HELSBY, F. W.: Mass Transfer in Liquid Gas Systems, with Special Reference to the Use of Foams. Ph. D. Thesis. Univ. of London (1958)
9. LOBO, W. E.—FRIEND, L.—HASHMALL, L.—ZENZ, F.: A. I. Ch. E. Tr. **41**, 693 (1945)
10. LARKING, R. P.—WHITE, R. R.—JEFFREY, D. W.: A. I. Ch. E. Journal **7**, 231 (1961)
11. LAPIDUS, L.: Ind. Eng. Chem. **49**, 1000 (1957)
12. WEEKMAN, V. W.—MYERS, J. E.: A. I. Ch. E. Journal **10**, 951 (1964)
13. WEBER, H. H.: Untersuchungen über die Verweilzeit-Verteilung in Aufstrom-Kolonnen. Dissertation. Technische Hochschule Darmstadt, Germany (1961)
14. SAADA, M. Y.: Génie Chimique **102**, 1283 (1969)

Prof. Mahmoud Y. SAADA, Pilot Plant Laboratories, National Research Centre,
Dokki, Cairo, U.A.R.